



Technical note: A new online tool for $\delta^{18}\text{O}$ -temperature conversions

Daniel E. Gaskell¹, Pincelli M. Hull¹

¹Department of Earth & Planetary Sciences, Yale University, New Haven, CT 06511, USA

Correspondence to: Daniel E. Gaskell (daniel.gaskell@yale.edu)

5 **Abstract.** The stable oxygen isotopic composition of marine carbonates ($\delta^{18}\text{O}_c$) is one of the oldest and most widely-used paleothermometers, but interpretation of these data is complicated by the necessity of knowing the $\delta^{18}\text{O}$ of the source seawater ($\delta^{18}\text{O}_w$). The effect of local hydrography (the “salinity effect”) is particularly difficult to correct for and may lead to errors of >10°C in sea-surface temperatures if neglected. A variety of methods for calculating $\delta^{18}\text{O}_w$ have been developed in the literature, but not all are readily accessible to workers. Likewise, temperature estimates are sensitive to a range of other calibration choices (such as calibration species and the inclusion or exclusion of carbonate ion effects) which can require significant effort to intercompare. We present an online tool for $\delta^{18}\text{O}$ -temperature conversions which provides convenient access to a wide range of calibrations and methods from the literature. Using results from recent isotope-enabled climate simulations, we show that the common method of estimating $\delta^{18}\text{O}_w$ from sample latitudes likely results in paleotemperature estimates that are too cold by up to 5°C in the North Atlantic and too hot by up to 5°C in the Southern Ocean during the warmest climate states. Our tool provides a convenient way for workers to examine the effects of alternate calibration and correction procedures on their $\delta^{18}\text{O}$ -based temperature estimates.

1 Motivation

The stable oxygen isotopic composition of carbonates ($\delta^{18}\text{O}_c$) is one of the oldest and most widely-used paleothermometers and undergirds a wide variety of paleoceanographic research (for recent reviews, see Pearson, 2012; Sharp, 2017). Converting $\delta^{18}\text{O}_c$ to temperature is typically done using an empirical calibration such as

$$T = 16.5 - 4.80(\delta^{18}\text{O}_c - \delta^{18}\text{O}_w - 0.27), \quad (1)$$

(Bemis et al., 1998), where T is temperature (in °C), $\delta^{18}\text{O}_c$ is the oxygen isotope composition of the carbonate (as ‰ VPDB), and $\delta^{18}\text{O}_w$ is the oxygen isotope composition of the water in which the carbonate was precipitated (as ‰ VSMOW). Much of the complexity of using $\delta^{18}\text{O}$ as a paleothermometer arises from the need to know $\delta^{18}\text{O}_w$, which may vary both globally as a function of sea level and locally at the sea surface as a function of regional hydrography (Sharp, 2017). Global variation can be estimated using independent records of sea level, so the global record of deep-water $\delta^{18}\text{O}$ -based temperatures has been relatively well-established (Zachos et al., 2001; Cramer et al., 2009; Westerhold et al., 2020; Rohling et al., 2021; etc.) However, local variations in surface $\delta^{18}\text{O}_w$ are more difficult to predict, rendering sea-surface temperature (SST) estimates



from $\delta^{18}\text{O}$ less reliable than deep-water temperature estimates. To address this, a variety of methods have been developed in
30 the literature to estimate surface $\delta^{18}\text{O}_w$.

Since modern surface $\delta^{18}\text{O}_w$ broadly covaries with latitude, a common approach has been to apply the modern latitudinal
variation to a sample's paleolatitude (typically using the relationship fit from Southern Ocean data in Zachos et al., 1994 Eq.
1; or more recently the updated method of Hollis et al., 2019). However, this approach performs poorly in the North Atlantic
and other high northern latitudes, where local $\delta^{18}\text{O}_w$ can deviate significantly from the latitudinal mean (Fig. 1; Zachos et al.,
35 1994; Gaskell et al., 2022; see also generally Tindall et al., 2010). It also assumes that the latitudinal gradient in $\delta^{18}\text{O}_w$ has not
changed through time, which is contradicted by modeling. In warmer climates with an altered hydrological cycle, models
predict that regional salinity contrasts should change (Richter and Xie, 2010; Singh et al., 2016), with an analogous effect on
 $\delta^{18}\text{O}_w$ (Zhou et al., 2008; Tindall et al., 2010; Roberts et al., 2011; Zhu et al., 2020). In particularly extreme cases such as the
Eocene, the theoretical difference between modern latitude-derived $\delta^{18}\text{O}_w$ (after Zachos et al., 1994 Eq. 1) and modeled local
40 $\delta^{18}\text{O}_w$ at 6x preindustrial $p\text{CO}_2$ (Zhu et al., 2020) yields a mean temperature error of 5 °C in the Southern Ocean (60–90 °S) or
an astonishing mean temperature error of 41 °C above the Arctic Circle (66.5–90 °N; Figure 1).

An alternative approach is to obtain $\delta^{18}\text{O}_w$ more or less directly from isotope-enabled climate models (Zhou et al., 2008;
Roberts et al., 2011; Gaskell et al., 2022). Several approaches have been adopted: drawing local $\delta^{18}\text{O}_w$ directly from model
output (Roberts et al., 2011); using modeled zonal mean $\delta^{18}\text{O}_w$ for a particular paleolatitude (Zhou et al., 2008); using models
45 as input to fit a generalized equation for predicting $\delta^{18}\text{O}_w$ from latitude and bottom-water temperature (Gaskell et al., 2022 Eq.
S9); or, recently, a generalized method which uses bottom-water temperature to interpolate local $\delta^{18}\text{O}_w$ between models run at
different $p\text{CO}_2$ (Gaskell et al., 2022). While some authors have avoided these approaches altogether due to the uncertainty of
modeled $\delta^{18}\text{O}_w$ (e.g., Hollis et al., 2012) or the possibility of introducing circularity into data-model comparisons (e.g., Hollis
et al., 2019), model-derived $\delta^{18}\text{O}_w$ clearly captures information lost by simpler approaches and is therefore appropriate for
50 some use-cases (Roberts et al., 2011).

Here, we present a new online tool for $\delta^{18}\text{O}$ temperature conversion which automates a range of methods for $\delta^{18}\text{O}_w$
reconstruction and correction from the literature, improving the accessibility of advanced methods to workers generating $\delta^{18}\text{O}_c$
data. We show that the selection of conversion methodology can have a significant impact on the interpretation of the resulting
temperatures, particularly those from warm climate states.

55 2 Description

We present a new online tool for performing $\delta^{18}\text{O}_c$ -temperature conversions which automates a range of methods from the
literature. A preprint version of this tool is available at <https://www.danielgaskell.com/d18O> [NOTE: This URL will be updated
to a permanent institutional URL for publication.] After uploading a datasheet of $\delta^{18}\text{O}_c$ measurements, users may select from
one of 63 different calibrations from the literature (e.g., Bemis et al., 1998; Kim and O'Neil, 1997; Malevich et al., 2019;
60 Marchitto et al., 2014; etc.). Calibrations are standardized to express $\delta^{18}\text{O}_c$ in units of ‰ VPDB and $\delta^{18}\text{O}_w$ in units of ‰



VSMOW, following the methods used to construct the original calibrations. Users may then select one of 15 different methods or records for estimating global $\delta^{18}\text{O}_w$ from the literature (e.g., Cramer et al., 2011; Miller et al., 2020; Rohling et al., 2021; full list in supplementary material). All built-in calibration records are internally converted to four different timescales, so the user can select the timescale consistent with their data: GTS2004 (Gradstein et al., 2005), GTS2012 (Gradstein et al., 2012),
65 GTS2016 (Ogg et al., 2016), and GTS2020 (Gradstein et al., 2020). These timescale conversions are performed by linear interpolation between magnetochron boundaries; dataset files can be found on the project GitHub.

The user may then select a method for estimating local $\delta^{18}\text{O}_w$. These are as follows: performing no local correction; using modern $\delta^{18}\text{O}_w$ from each sample's location and a specified depth (after LeGrande and Schmidt, 2006); using reconstructed Late Holocene or Last Glacial Maximum surface $\delta^{18}\text{O}_w$ from each sample's location (after Tierney et al., 2020); using $\delta^{18}\text{O}_w$
70 estimated from latitude alone (after Zachos et al., 1994 Eq. 1; or the method of Hollis et al., 2019); using $\delta^{18}\text{O}_w$ estimated from latitude and bottom-water temperature (after Gaskell et al., 2022 Eq. S9); or using $\delta^{18}\text{O}_w$ estimated from isotope-enabled climate models (after the method of Gaskell et al., 2022, presently provided using datasets of Miocene and Eocene paleogeography). For methods which draw from an existing dataset of $\delta^{18}\text{O}_w$, the user may specify a number of degrees latitude/longitude to average over in order to capture a regional mean when the exact paleocoordinates or local hydrography
75 may not be known. To help determine site locations at the time of deposition, an option is also provided to automatically perform paleocoordinate rotations using the GPLates Web Service (Müller et al., 2018).

Because $\delta^{18}\text{O}_c$ is known to vary with aqueous carbonate chemistry (the “carbonate ion effect”; Spero et al., 1997; Bijma et al., 1999; Ziveri et al., 2012), users may also specify a carbonate ion correction factor. This is performed by adjusting $\delta^{18}\text{O}_c$ with the linear relationship

$$80 \quad \delta^{18}\text{O}'_c = \delta^{18}\text{O}_c - (s[\text{CO}_3^{2-}] - 200s), \quad (2)$$

where $\delta^{18}\text{O}_c$ is the uncorrected oxygen isotope composition of the carbonate, $\delta^{18}\text{O}'_c$ is the corrected oxygen isotope composition of the carbonate, s is the selected slope of the effect (in ‰ VPDB per $\mu\text{mol L}^{-1} \text{CO}_3^{2-}$), and $[\text{CO}_3^{2-}]$ is the concentration of carbonate ion in solution (in $\mu\text{mol kg}^{-1}$). This relationship yields no correction when $[\text{CO}_3^{2-}] = 200 \mu\text{mol kg}^{-1}$, an approximation of the mean modern surface value (after the long-term record of Zeebe and Tyrrell, 2019). The user may
85 specify $[\text{CO}_3^{2-}]$ manually or select a published long-term record of $[\text{CO}_3^{2-}]$ (Tyrrell and Zeebe, 2004; Zeebe and Tyrrell, 2019). On completion, the tool presents a formatted table of the resulting temperatures, along with any intermediate values (such as estimated $\delta^{18}\text{O}_w$) which were required to generate them. Any rows with errors (e.g., paleocoordinates which do not yield a valid $\delta^{18}\text{O}_w$ estimate) are flagged with a warning. For reference, a short summary of methods is also generated, including relevant equations and a complete bibliography of citations for the methods employed in each run.



90 3 Demonstration of the effect of $\delta^{18}\text{O}_w$ -reconstruction methods

3.1 Data and methods

To illustrate the effects of differing methods of reconstructing $\delta^{18}\text{O}_w$, we apply a range of methods to reported site mean $\delta^{18}\text{O}_c$ from planktonic foraminifera in the DeepMIP 0.1 proxy database (Hollis et al., 2019). Because $\delta^{18}\text{O}_c$ in planktonic foraminifera is strongly susceptible to diagenetic alteration (Pearson et al., 2001), we use only sites with “glassy” preservation. All
95 temperature conversions are performed using our tool described above, using paleocoordinates reported in the original publication and selecting GTS2012 age datums (Gradstein et al., 2012), the *Orbulina universa* low-light calibration (Bemis et al., 1998), and a global $\delta^{18}\text{O}_w$ record based on bottom-water Mg/Ca temperatures (Miller et al., 2020). We do not perform a carbonate ion effect correction due to a lack of data on effect strengths in the Eocene.

We compare seven methods of estimating local $\delta^{18}\text{O}_w$: 1) no correction; 2) the mean modern value over 0-50 m depth (after
100 LeGrande and Schmidt, 2006); 3) the reconstructed surface value at the Last Glacial Maximum (after Tierney et al., 2020); 4) the traditional latitude-only method (Zachos et al., 1994 Eq. 1); 5) the updated latitude-based method of Hollis et al. (2019); 6) the latitude-and-bottom-water-temperature method of Gaskell et al. (2022) Eq. S9; and 7) the climate-model-based method of Gaskell et al. (2022), with Eocene paleogeography (CESMv1.2-CAM5 model dataset with 1x, 3x, 6x, and 9x preindustrial pCO₂, after Zhu et al., 2020). Where applicable, mean values are taken from $\pm 5^\circ$ latitude/longitude around each site’s
105 paleocoordinates and bottom-water temperatures are taken from the Mg/Ca-based record of Miller et al. (2020). For PETM intervals, a bottom-water temperature of 17.75 °C (4 °C over latest Paleocene temperatures; Tripathi and Elderfield, 2005) is assumed as the full magnitude of warming is not captured in the Miller et al. (2020) temperature record. Note that using Eocene paleocoordinates directly to obtain $\delta^{18}\text{O}_w$ estimates from datasets with Quaternary paleogeography (methods #2 and #3) is not strictly appropriate and leads to some sites being omitted due to their paleocoordinates falling over land. In a realistic scenario
110 only methods with appropriate paleogeography should be used.

For comparison with other proxy estimates, we paired each site with the geographically nearest site (by great circle distance) for which Mg/Ca and TEX₈₆ temperature estimates are reported in the DeepMIP v0.1 compilation and then, for each site, calculated the residual between the $\delta^{18}\text{O}$ -based temperature and the mean of Mg/Ca and TEX₈₆ temperatures. Sites lacking matching Mg/Ca and TEX₈₆ temperature estimates within a 1650 km radius were omitted, leaving four sites from the North
115 Atlantic: DSDP 401, Bass River, Wilson Lake, and Millville.

3.2 Results

Choice of $\delta^{18}\text{O}_w$ -reconstruction method induces variations in site temperatures with an average standard deviation of 1.5 °C across all sites (i.e., approximately ± 3.0 °C error at the 2 σ or 95% level). As would be expected from Figure 1, spatially-explicit methods yield higher temperatures than those relying on paleolatitude alone for most sites in the Atlantic, but lower
120 temperatures for sites in the Pacific and Indian Oceans. The updated latitudinal method of Hollis et al. (2019) yields colder temperatures at all sites than the older method of Zachos et al. (1994) Eq. 1, due primarily to differences in predicted Northern



Hemisphere $\delta^{18}\text{O}_w$. Comparisons between $\delta^{18}\text{O}$ -based and Mg/Ca+TEX₈₆-based temperatures is shown in Figure 3. Using the spatially-explicit Gaskell et al. (2022) method produces results that are significantly closer to with Mg/Ca+TEX₈₆-based temperatures than the latitudinal method (Hollis et al., 2019) employed by the original DeepMIP v0.1 proxy compilation (F-test of residuals, $p = 0.036$), but are not significantly different from results obtained using the method of Zachos et al. (1994) Eq. 1 ($p = 0.227$).

4 Concluding remarks

Our tool provides a convenient way for workers to perform $\delta^{18}\text{O}$ -temperature conversions and explore the sensitivity of their results to different calibrations, corrections, and $\delta^{18}\text{O}_w$ -reconstruction methods. By allowing data-generators to rapidly generate multiple temperature estimates for their records with different underlying assumptions, our tool allows workers to quickly understand and quantify the effects of different assumptions on the resulting temperature estimates.

The demonstration included here suggests that reconstructing $\delta^{18}\text{O}_w$ from latitude alone can induce substantial errors and that spatially-explicit methods such as that proposed by Gaskell et al. (2022) can significantly improve correspondence between $\delta^{18}\text{O}$ -based temperatures and other proxy estimates, at least in the North Atlantic. However, it should be noted that at high latitudes during the warmest time intervals, $\delta^{18}\text{O}$ can yield temperatures 5–10 °C colder than those predicted by other proxies (e.g., Zhu et al., 2019; Gaskell et al., 2022). If models are correct in their predictions that warmer climate states can result in significantly depleted high-latitude $\delta^{18}\text{O}_w$ (Zhou et al., 2008; Tindall et al., 2010; Roberts et al., 2011; Zhu et al., 2020), then using model-based methods to reconstruct $\delta^{18}\text{O}_w$ would only increase this discrepancy further. Improving our understanding of $\delta^{18}\text{O}_w$ changes in warm climate states is therefore an important component of resolving ongoing proxy discrepancies in the high latitudes.

Code availability

An online version of the most current release of our tool is maintained at <https://www.danielgaskell.com/d18O> [preprint URL, subject to change]. Source code (Javascript and PHP) is available from the project's GitHub repository at <https://github.com/danielgaskell/d18Oconverter>.

References

Bemis, B. E., Spero, H. J., Bijma, J., and Lea, D. W.: Reevaluation of the oxygen isotopic composition of planktonic foraminifera: Experimental results and revised paleotemperature equations, *Paleoceanography*, 13, 150–160, <https://doi.org/10.1029/98PA00070>, 1998.



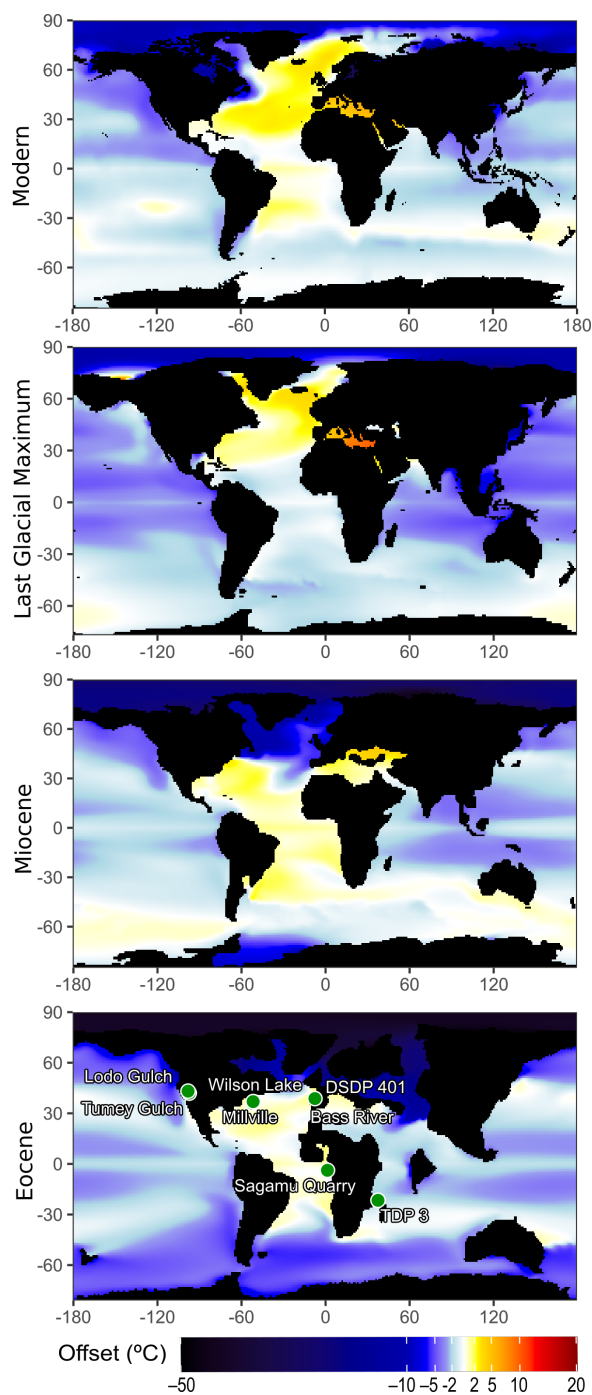
- 150 Bijma, J., Spero, H. J., and Lea, D. W.: Reassessing Foraminiferal Stable Isotope Geochemistry: Impact of the Oceanic Carbonate System (Experimental Results), in: Use of Proxies in Paleoceanography, edited by: Fischer, D. G. and Wefer, P. D. G., Springer Berlin Heidelberg, 489–512, https://doi.org/10.1007/978-3-642-58646-0_20, 1999.
- Cramer, B. S., Toggweiler, J. R., Wright, J. D., Katz, M. E., and Miller, K. G.: Ocean overturning since the Late Cretaceous: Inferences from a new benthic foraminiferal isotope compilation, *Paleoceanography*, 24, PA4216, <https://doi.org/10.1029/2008PA001683>, 2009.
- 155 Cramer, B. S., Miller, K. G., Barrett, P. J., and Wright, J. D.: Late Cretaceous–Neogene trends in deep ocean temperature and continental ice volume: Reconciling records of benthic foraminiferal geochemistry ($\delta^{18}\text{O}$ and Mg/Ca) with sea level history, *Journal of Geophysical Research: Oceans*, 116, <https://doi.org/10.1029/2011JC007255>, 2011.
- Gaskell, D. E., Huber, M., O’Brien, C. L., Inglis, G. N., Acosta, R. P., Poulsen, C. J., and Hull, P. M.: The latitudinal temperature gradient and its climate dependence as inferred from foraminiferal $\delta^{18}\text{O}$ over the past 95 million years, *Proceedings of the National Academy of Sciences*, 119, e2111332119, <https://doi.org/doi:10.1073/pnas.2111332119>, 2022.
- 160 Gradstein, F. M., Ogg, J. G., and Smith, A. G. (Eds.): *A Geologic Time Scale 2004*, Cambridge University Press, Cambridge, <https://doi.org/10.1017/CBO9780511536045>, 2005.
- Gradstein, F. M., Ogg, J. G., Schmitz, M. D., and Ogg, G. M. (Eds.): *The Geologic Time Scale*, Elsevier, <https://doi.org/10.1016/C2011-1-08249-8>, 2012.
- 165 Gradstein, F. M., Ogg, J. G., Schmitz, M. D., and Ogg, G. M.: *Geologic Time Scale 2020*, Elsevier, San Diego, NETHERLANDS, THE, 2020.
- Hollis, C. J., Taylor, K. W. R., Handley, L., Pancost, R. D., Huber, M., Creech, J. B., Hines, B. R., Crouch, E. M., Morgans, H. E. G., Crampton, J. S., Gibbs, S., Pearson, P. N., and Zachos, J. C.: Early Paleogene temperature history of the Southwest Pacific Ocean: Reconciling proxies and models, *Earth and Planetary Science Letters*, 349–350, 53–66, <https://doi.org/10.1016/j.epsl.2012.06.024>, 2012.
- 170 Hollis, C. J., Dunkley Jones, T., Anagnostou, E., Bijl, P. K., Cramwinckel, M. J., Cui, Y., Dickens, G. R., Edgar, K. M., Eley, Y., Evans, D., Foster, G. L., Frieling, J., Inglis, G. N., Kennedy, E. M., Kozdon, R., Lauretano, V., Lear, C. H., Littler, K., Lourens, L., Meckler, A. N., Naafs, B. D. A., Pälike, H., Pancost, R. D., Pearson, P. N., Röhl, U., Royer, D. L., Salzmann, U., Schubert, B. A., Seebeck, H., Sluijs, A., Speijer, R. P., Stassen, P., Tierney, J., Tripathi, A., Wade, B., Westerhold, T., Witkowski, C., Zachos, J. C., Zhang, Y. G., Huber, M., and Lunt, D. J.: The DeepMIP contribution to PMIP4: methodologies for selection, compilation and analysis of latest Paleocene and early Eocene climate proxy data, incorporating version 0.1 of the DeepMIP database, *Geoscientific Model Development*, 12, 3149–3206, <https://doi.org/10.5194/gmd-12-3149-2019>, 2019.
- Kim, S.-T. and O’Neil, J. R.: Equilibrium and nonequilibrium oxygen isotope effects in synthetic carbonates, *Geochimica et Cosmochimica Acta*, 61, 3461–3475, [https://doi.org/10.1016/S0016-7037\(97\)00169-5](https://doi.org/10.1016/S0016-7037(97)00169-5), 1997.
- 180 LeGrande, A. N. and Schmidt, G. A.: Global gridded data set of the oxygen isotopic composition in seawater, *Geophysical Research Letters*, 33, <https://doi.org/10.1029/2006GL026011>, 2006.
- Malevich, S. B., Vetter, L., and Tierney, J. E.: Global Core Top Calibration of $\delta^{18}\text{O}$ in Planktic Foraminifera to Sea Surface Temperature, *Paleoceanography and Paleoclimatology*, 34, 1292–1315, <https://doi.org/10.1029/2019PA003576>, 2019.
- 185 Marchitto, T. M., Curry, W. B., Lynch-Stieglitz, J., Bryan, S. P., Cobb, K. M., and Lund, D. C.: Improved oxygen isotope temperature calibrations for cosmopolitan benthic foraminifera, *Geochimica et Cosmochimica Acta*, 130, 1–11, <https://doi.org/10.1016/j.gca.2013.12.034>, 2014.



- Miller, K. G., Browning, J. V., Schmelz, W. J., Kopp, R. E., Mountain, G. S., and Wright, J. D.: Cenozoic sea-level and cryospheric evolution from deep-sea geochemical and continental margin records, *Science Advances*, 6, eaaz1346, <https://doi.org/10.1126/sciadv.aaz1346>, 2020.
- 190 Müller, R. D., Cannon, J., Qin, X., Watson, R. J., Gurnis, M., Williams, S., Pfaffelmoser, T., Seton, M., Russell, S. H. J., and Zahirovic, S.: GPlates: Building a Virtual Earth Through Deep Time, *Geochemistry, Geophysics, Geosystems*, 19, 2243–2261, <https://doi.org/10.1029/2018GC007584>, 2018.
- Ogg, J. G., Ogg, G. M., and Gradstein, F. M.: *A Concise Geologic Time Scale*, Elsevier, <https://doi.org/10.1016/C2009-0-64442-1>, 2016.
- 195 Pearson, P. N.: Oxygen Isotopes in Foraminifera: Overview and Historical Review, in: *Reconstructing Earth's Deep-Time Climate—The State of the Art in 2012*, Paleontological Society Short Course, vol. 18, The Paleontological Society, 1–38, 2012.
- Pearson, P. N., Ditchfield, P. W., Singano, J., Harcourt-Brown, K. G., Nicholas, C. J., Olsson, R. K., Shackleton, N. J., and Hall, M. A.: Warm tropical sea surface temperatures in the Late Cretaceous and Eocene epochs, *Nature*, 413, 481–487, <https://doi.org/10.1038/35097000>, 2001.
- 200 Richter, I. and Xie, S.-P.: Moisture transport from the Atlantic to the Pacific basin and its response to North Atlantic cooling and global warming, *Clim Dyn*, 35, 551–566, <https://doi.org/10.1007/s00382-009-0708-3>, 2010.
- Roberts, C. D., LeGrande, A. N., and Tripathi, A. K.: Sensitivity of seawater oxygen isotopes to climatic and tectonic boundary conditions in an early Paleogene simulation with GISS ModelE-R, *Paleoceanography*, 26, <https://doi.org/10.1029/2010PA002025>, 2011.
- 205 Rohling, E. J., Yu, J., Heslop, D., Foster, G. L., Opdyke, B., and Roberts, A. P.: Sea level and deep-sea temperature reconstructions suggest quasi-stable states and critical transitions over the past 40 million years, *Science Advances*, 7, eabf5326, <https://doi.org/10.1126/sciadv.abf5326>, 2021.
- Sharp, Z.: *Principles of Stable Isotope Geochemistry*, 2nd Edition, 2nd ed., University of New Mexico Open Textbooks, 416 pp., 2017.
- 210 Singh, H. K. A., Donohoe, A., Bitz, C. M., Nusbaumer, J., and Noone, D. C.: Greater aerial moisture transport distances with warming amplify interbasin salinity contrasts, *Geophysical Research Letters*, 43, 8677–8684, <https://doi.org/10.1002/2016GL069796>, 2016.
- Spero, H. J., Bijma, J., Lea, D. W., and Bemis, B. E.: Effect of seawater carbonate concentration on foraminiferal carbon and oxygen isotopes, *Nature*, 390, 497–500, <https://doi.org/10.1038/37333>, 1997.
- 215 Tierney, J. E., Zhu, J., King, J., Malevich, S. B., Hakim, G. J., and Poulsen, C. J.: Glacial cooling and climate sensitivity revisited, *Nature*, 584, 569–573, <https://doi.org/10.1038/s41586-020-2617-x>, 2020.
- Tindall, J., Flecker, R., Valdes, P., Schmidt, D. N., Markwick, P., and Harris, J.: Modelling the oxygen isotope distribution of ancient seawater using a coupled ocean–atmosphere GCM: Implications for reconstructing early Eocene climate, *Earth and Planetary Science Letters*, 292, 265–273, <https://doi.org/10.1016/j.epsl.2009.12.049>, 2010.
- 220 Tripathi, A. and Elderfield, H.: Deep-Sea Temperature and Circulation Changes at the Paleocene-Eocene Thermal Maximum, *Science*, 308, 1894–1898, <https://doi.org/10.1126/science.1109202>, 2005.

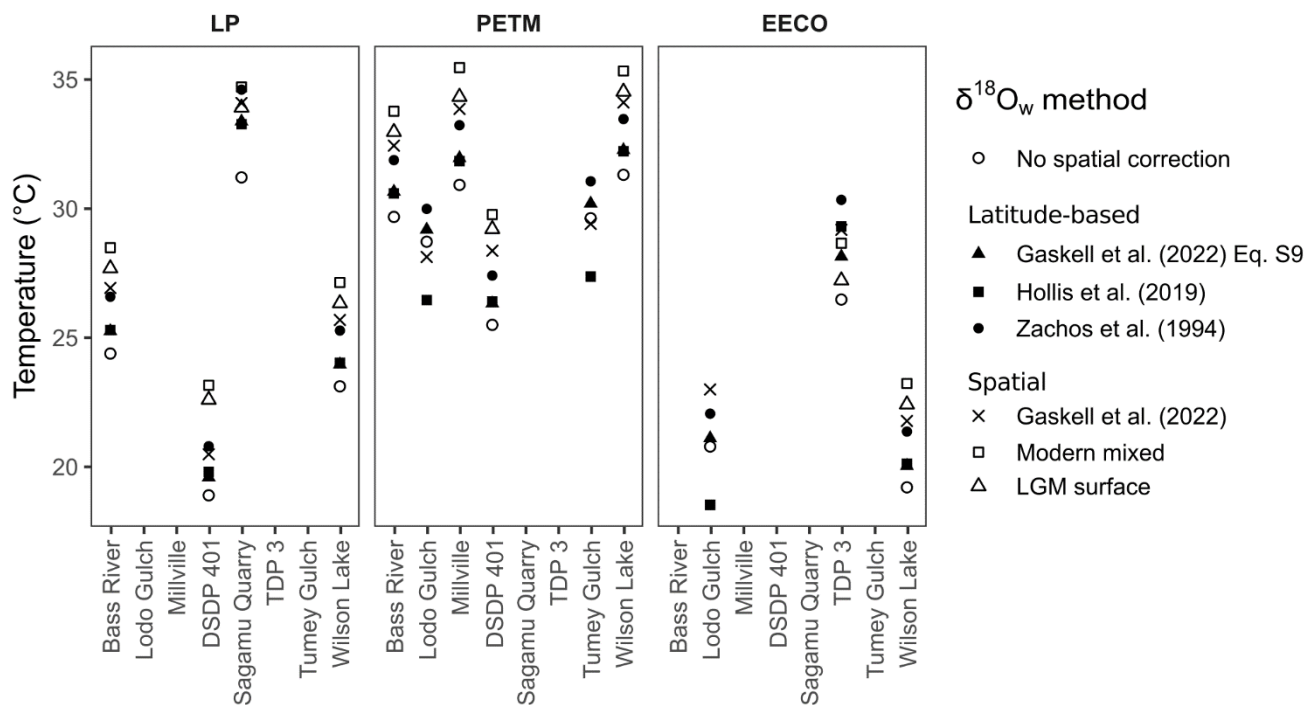


- Tyrrell, T. and Zeebe, R. E.: History of carbonate ion concentration over the last 100 million years, *Geochimica et Cosmochimica Acta*, 68, 3521–3530, <https://doi.org/10.1016/j.gca.2004.02.018>, 2004.
- 225 Westerhold, T., Marwan, N., Drury, A. J., Liebrand, D., Agnini, C., Anagnostou, E., Barnet, J. S. K., Bohaty, S. M., Vleeschouwer, D. D., Florindo, F., Frederichs, T., Hodell, D. A., Holbourn, A. E., Kroon, D., Laurentano, V., Littler, K., Lourens, L. J., Lyle, M., Pälike, H., Röhl, U., Tian, J., Wilkens, R. H., Wilson, P. A., and Zachos, J. C.: An astronomically dated record of Earth's climate and its predictability over the last 66 million years, *Science*, 369, 1383–1387, <https://doi.org/10.1126/science.aba6853>, 2020.
- 230 Zachos, J., Pagani, M., Sloan, L., Thomas, E., and Billups, K.: Trends, Rhythms, and Aberrations in Global Climate 65 Ma to Present, *Science*, 292, 686–693, <https://doi.org/10.1126/science.1059412>, 2001.
- Zachos, J. C., Stott, L. D., and Lohmann, K. C.: Evolution of Early Cenozoic marine temperatures, *Paleoceanography*, 9, 353–387, <https://doi.org/10.1029/93PA03266>, 1994.
- Zeebe, R. E. and Tyrrell, T.: History of carbonate ion concentration over the last 100 million years II: Revised calculations and new data, *Geochimica et Cosmochimica Acta*, <https://doi.org/10.1016/j.gca.2019.02.041>, 2019.
- Zhou, J., Poulsen, C. J., Pollard, D., and White, T. S.: Simulation of modern and middle Cretaceous marine $\delta^{18}\text{O}$ with an ocean-atmosphere general circulation model, *Paleoceanography*, 23, <https://doi.org/10.1029/2008PA001596>, 2008.
- Zhu, J., Poulsen, C. J., and Tierney, J. E.: Simulation of Eocene extreme warmth and high climate sensitivity through cloud feedbacks, *Science Advances*, 5, eaax1874, <https://doi.org/10.1126/sciadv.aax1874>, 2019.
- 240 Zhu, J., Poulsen, C. J., Otto-Bliesner, B. L., Liu, Z., Brady, E. C., and Noone, D. C.: Simulation of early Eocene water isotopes using an Earth system model and its implication for past climate reconstruction, *Earth and Planetary Science Letters*, 537, 116164, <https://doi.org/10.1016/j.epsl.2020.116164>, 2020.
- Ziveri, P., Thoms, S., Probert, I., Geisen, M., and Langer, G.: A universal carbonate ion effect on stable oxygen isotope ratios in unicellular planktonic calcifying organisms, *Biogeosciences*, 9, 1025–1032, <https://doi.org/10.5194/bg-9-1025-2012>, 2012.
- 245

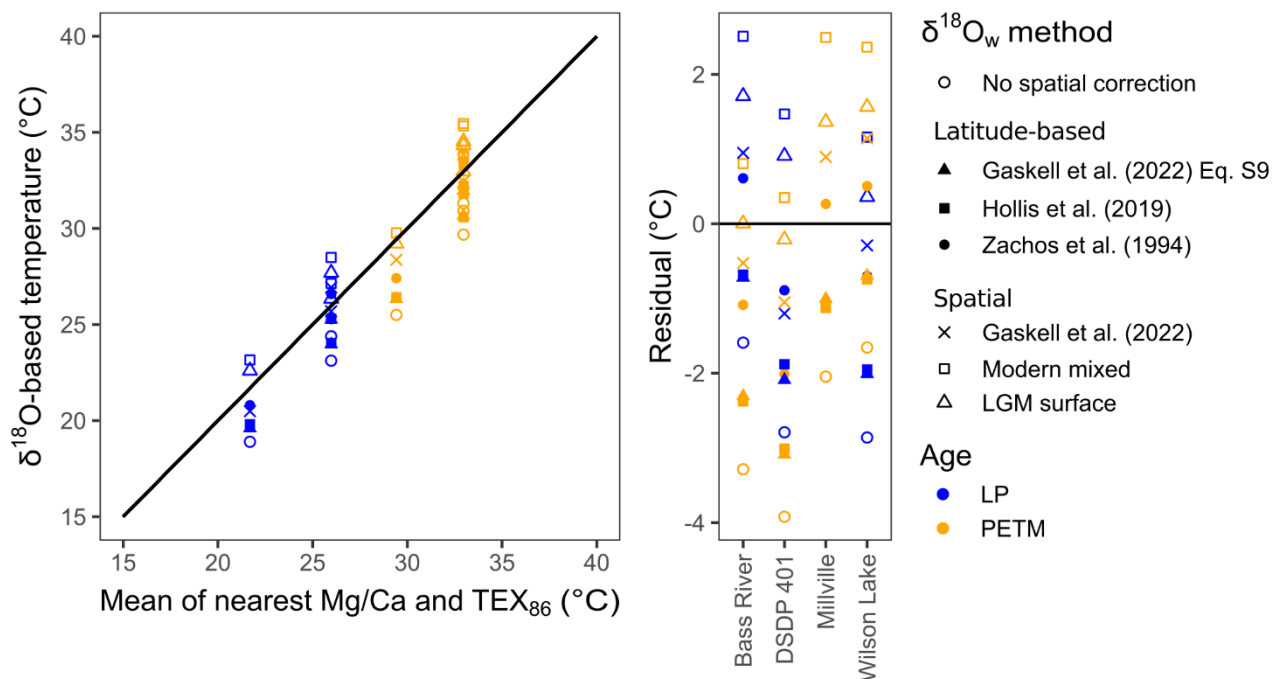


250

Figure 1: Effect of estimating SST using measured/modelled local $\delta^{18}\text{O}_w$ rather than the latitude-based approximation of Zachos et al. (1994) Eq. 1. Modern: comparison with mean annual $\delta^{18}\text{O}_w$ <50 m depth (after LeGrande and Schmidt, 2006). Last Glacial Maximum (LGM): comparison with inferred annual surface $\delta^{18}\text{O}_w$ at the LGM (Tierney et al., 2020). Miocene: comparison with CESMv1.2_CAM5 model run at 400 ppm CO_2 with Miocene paleogeography (Gaskell et al., 2022). Eocene: comparison with CESM_1.2_CAM5 model run at 6x preindustrial CO_2 with Eocene paleogeography (Zhu et al., 2020). Temperatures are calculated assuming a slope of $4.80\text{ }^\circ\text{C}\text{ }^\circ\text{ }^{-1}$ (Bemis et al., 1998).



255 **Figure 2: DeepMIP v0.1 δ¹⁸O sites converted to temperature after the seven methods described in the text. Age groupings follow the original publication (LP = Latest Paleocene, PETM = Paleocene-Eocene Thermal Maximum, EECO = Early Eocene Climate Optimum; Hollis et al., 2019).**



260

Figure 3: Comparison of $\delta^{18}\text{O}$ -based temperatures with the mean of the geographically nearest Mg/Ca and TEX_{86} -based temperatures from the DeepMIP v0.1 proxy compilation.